Sensors & Transducers, Vol. 207, Issue 12, December 2016, pp. 44-49

www.sensorsportal.com

Sensors & Transducers

Published by IFSA Publishing, S. L., 2016
http://www.sensorsportal.com

Vector Magnetometer Application with Moving Carriers

Andrii PRYSTAI, Valery KOREPANOV, Fedir DUDKIN and Borys LADANIVSKYY

LLC Laboratory for Electromagnetic Innovations (LEMI), 5-A Naukova Str., Lviv, 79060, Ukraine
Tel.: + 380322639163, fax: + 380322639163
E-mail: vakor@isr.lviv.ua

Received: 5 November 2016 /Accepted: 5 December 2016 /Published: 30 December 2016

Abstract: In magnetic prospecting the aeromagnetic survey is a widespread method used for research in large territories or in the areas with difficult access (forests, swamps, shallow waters). At present, a new type of mobile carriers – remotely piloted vehicles or drones – is becoming very common. The drones supplied by magnetometer can be also used for underground utility location (for example, steel and concrete constructions, buried power cables, to name a few). For aeromagnetic survey, obtaining of 3-component magnetic field data gives higher processing precision, so the fluxgate magnetometers (FGM) seem to be the most preferable by reason of low weight, noise, power consumption and costs. During movement of FGM fixed to a drone practically permanent attitude changes in the Earth's magnetic field arises with corresponding changes of its projection at FGM axes. Also the electromagnetic interference from the drone motor and uncontrolled oscillations of drone and suspension are the factors which limit the magnetometer sensitivity level. Aroused because of this, signals significantly exceed the expected signals from a studied object and so should be removed by proper interference filtration and use of stabilized towed construction, as well as at data processing. To find the necessary resolution threshold of a drone-portable FGM, the modeling was made to estimate magnetic field value from a small sphere about 1 cm radius at the minimal altitude of drone flight and it was shown that such a small object can be reliably detected if the FGM noise level is less than 0.15 nT. Next requirement is the necessity to decrease as much as possible the FGM power consumption with retention of low noise level. Finally, because of drone movement, the broadening of a frequency range should be done. The LEMI-026 magnetometer was developed satisfying all requirements to the drone-mounted device. The field tests were successfully performed using two of LEMI-026 magnetometers and it was concluded that the parameters of these magnetometers allow their using for the magnetic survey with moving platforms.

Keywords: Drone, Flux-gate magnetometer, Aeromagnetic survey, Modeling, Test results.

1. Introduction

Geological/geophysical prospecting magnetometry is widely used method which is based on the difference in the magnetic properties of soils and rocks (see, for example, [1]). Magnetic prospecting studies the magnetic anomalies produced by geological bodies that have been magnetized by present-day (induced magnetization) and ancient (residual magnetization) geomagnetic fields. Their magnetization is determined by the presence of ferromagnetic minerals (for example, magnetite, pyrrhotite). In magnetic prospecting the aeromagnetic survey is a widespread method for large territories or in the areas with difficult access (forests, swamps, shallow waters).

Till recently, it was realized mostly with specialized planes and helicopters. At present, a new type of such carriers – remotely piloted vehicles or

drones – is becoming more common. Additionally to the mining exploration and regional geophysical studies, they allow solving much wider spectrum of tasks. For example, it is a location of the archeological sites, where the alteration and concentration of weakly magnetic minerals to fine grained iron oxides, such as magnetite or maghaemite, during human activity lead to the increase of soil magnetic susceptibility [2-4]. The soil magnetic properties mapping is necessary for: application of soil compensation techniques for the detection of buried metallic objects (UXO, EOD, landmines etc.) using electromagnetic sensors; study the effect of small scale spatial variation of soil magnetic susceptibility [5-6]. Digital soil mapping can contribute significantly to prediction of the soil spatial and parameter distribution in the landscape using models. Initially soils were mapped as class maps (i. e. soil types) but increasingly property maps can be developed, [7-8]. The wetlands aeromagnetic inspection with drones is applicable for archaeology, agriculture and civil works [2, 9-12]. Metal debris and contamination detection are required at landfill mining and reclamation when wastes (metal debris and scrap) and contaminated by heavy metals soil are excavated and processed at soil remediation [13-15]. Also drones supplied by magnetometer can be used for underground utility location (for example, steel and concrete constructions, buried DC and AC power cables, to name a few). For these purposes the magnetometer with frequency range DC-AC up to 60 Hz is necessary [16-18].

The magnetic field of buried detected/located objects or soil inhomogeneities is too weak, even in close proximity of the earth's surface, and needs for reliable detection very sensitive magnetometers. Also at surveying of large areas a mobile lightweight device for productive and low cost measurements is necessary. Now, at magnetic prospecting the most used are the scalar magnetometers which have a very high sensitivity and some of them have a moderate mass for application with drones. For example, Cesium-vapor magnetometer G-822A has noise less than 0.001 nT/√Hz rms at a 0.1 second sample rate, sensor and electronic module weight 339 and 623 g respectively [19]. However, the scalar magnetometers have essential drawback because of absolute value magnetic field measurement, which limits the possibilities of data interpretation by application of methods for inverse problem solution.

For obtaining of 3-component magnetic field data, the fluxgate magnetometers (FGM) seem to be the most preferable by reason of low weight, noise, power consumption and costs. For example, FGM designed for drone application has noise less than 0.02 nT/√Hz rms at 1 Hz, sample rate 200 Hz, power consumption 6 W, sensor and electronic weight 200 and 500 g respectively [20]. There is no information about data collection system for this FGM, and its power consumption is too high for small portable batteries. So, the adaptation of FGMs for the measurement onboard such a small size and low-powered carriers implies further more stringent requirements to their technical parameters. Other hindrance, resulted from instability of FGM axes orientation and distance to boundary air-ground during magnetic prospecting, strongly impedes the measuring procedure and data interpretation [21]. This problem still waits for new theoretical investigations and experimental ideology, which will allow obtaining the final results with high accuracy.

2. Problems of FGM Application for Moving Carriers

During movement of suspended or fixed FGM on a drone practically permanent attitude changes in the Earth's magnetic field $\mathbf{B}_0$ arises. The corresponding changes of $\mathbf{B}_0$ projection on FGM axes significantly exceed the expected signal from a studied object and so should be removed at data processing. For example, the sensor deviation at as tiny angle as 0.01° may lead to the appearance of parasitic signal up to 5-12 pT. At the same time the minimal anomalous magnetic field at geomagnetic prospecting can be of value about

$$B_{\min} \sim kB_0 \approx 10^{-5} B_0 = 0.3 - 0.7 \text{ , pT,} \quad (1)$$

where κ is the soil magnetic susceptibility [22], $B_0=|\mathbf{B}_0|$.

The appropriate FGM orientation in flight is hardly ever can be controlled for such small carriers. Nevertheless, at geomagnetic prospecting, where the large areas with slow change of the soil magnetic susceptibility are studied, the measurement of anomalous magnetic field components is not so important because of absence of the pronounced structural configurations. Such a study can be provided by FGM in magnetic field absolute value measurement mode. The anomalous magnetic field value ΔB_i is calculated by simple equation

$$\Delta B_i = B_i - B_i \text{ , } \quad (2)$$

where B_1, B_i are the first and i-th magnetic field absolute value readings on the studied profile, $B_i = (B_{x,i}^2 + B_{y,i}^2 + B_{z,i}^2)^{0,5}$.

For such a case, the FGM orientation does not affect on ΔB_i estimation. And to distinguish temporal and spatial variations of the magnetic field, a stationary reference magnetometer with known orientation has to be installed in the area where the survey is executed.

At fast magnetic field changes, for example at buried compact object or UXO detection and classification the 3-component anomalous magnetic field measurements are obligatory. Very often for decreasing of air-ground boundary influence the gradiometric measurements are applied. In this case two FGMs are mounted on a rigid platform at fixed distance (see, for example, Magdrone II [20]).

To find the necessary resolution threshold of FGM for this purpose, let us estimate the magnetic field value at differential (gradiometric) detection method of a small steel sphere with radius R=1 cm and magnetic permeability $\mu_s=300\mu_0$, where μ_0 is magnetic permeability of free space ($\mu_0=4\pi\times10^{-7}$H/m). Because the sphere is small in comparison with distance r to the sensor we can use the dipole approximation for its induced field **B** in the Earth external magnetic field $\mathbf{B}_0$:

$$B = \mu_0(3r(M\cdot r)/r^5 - M/r^3)/4\pi \qquad (3)$$

The vector of magnetic moment **M** for steel sphere equals to [23]:

$$M = 4\pi R^3(\mu_s-\mu_0)B_0/(\mu_0(\mu_s+2\mu_0)) \qquad (4)$$

The results of arising anomalous magnetic fields calculation for movement of two FGMs placed on a boom with separation distance Δx=1 m over the steel sphere R=1 cm with centre coordinates $x_s=y_s=z_s=0$ at height z=0.5 m along x-direction (y=0) are shown in Figs. 1 - 2.

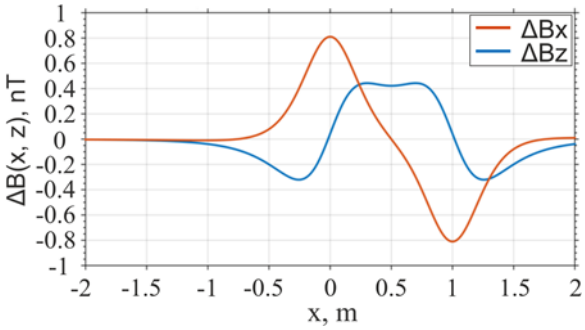

Fig. 1. Modeling results for a steel sphere with R=1 cm and Mx=My=0, Mz≠0 with centre coordinates xs=ys=zs=0, flight at height z=0.5 m along x-direction and B0, m=50,000 nT.

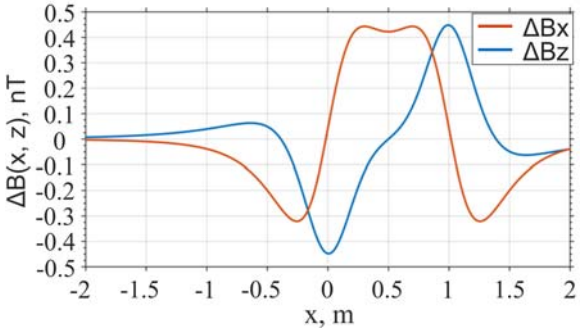

Fig. 2. Modeling results for a steel sphere with R=1 cm and My=Mz=0, Mx≠0 with centre coordinates xs=ys=zs=0, flight at height z=0.5 m along x-direction and B0, m=50,000 nT.

Here for simplification of numerical estimations we assume that $\mathbf{B}_0$ has direction along only one Cartesian coordinate axis m=x, y, z and its absolute value equals to B_0=50,000 nT. Thus anomalous magnetic field is calculated for two different magnetic moment orientations: $M_x=M_y=0$, $M_z\neq0$; $M_y=M_z=0$, $M_x\neq0$.

From these figures it is clearly seen that such a small object can be reliably detected if the FGM noise level is less than 0.15 nT. It should be noted that calculated anomalous fields is proportional to R^3, thus for steel sphere of R=2 cm the field maximums are in the range 3-6.4 nT. The same field intensity can be achieved at R=1 cm and z=0.25 m because of field proportionality to $1/r^3$.

3. Description of FGM for Drones

As it was stated above, FGM is the most suitable for vectorial magnetic field measurements with drones. That is why FGM was taken as basic magnetometer to be adapted to moving carrier applications. The most important parameter characterizing magnetometer quality is magnetic noise, which arises due to fluctuations determined by periodic magnetization of the FGM sensor core. For decrease the noise level, the attention has to be paid primarily to the selection of the best material for the sensor core, its annealing and excitation modes. Also, the proper selection of sensor housing material has to be made. It is assumed that the quality of electronic components used during FGM manufacturing allows neglecting their influence at the final FGM parameters. Taking into account very limited energetic capability of the drone, it is necessary to decrease as much as possible the FGM power consumption with retention of low noise level, which regularly increases with lowering of consumed power. Finally, because of drone movement, the broadening of a frequency range should be done because FGM usually are designed for measurement of very slow fluctuations (~DC-1 Hz).

The detailed analysis of the ways to fulfil necessary requirements to low power FGMs was presented in [24]. The use of recommendations given there allowed development of the customized FGM LEMI-026 which has several advantages relatively to best found in the publications drone-oriented FGM MagDrone One [20]. The comparison of technical parameters of these two FGMs is given in Table 1.

From this table it is evident that the developed magnetometer has strong advantages as to most important parameters – sensitivity threshold and especially power consumption. Also from the published parameters one may conclude that MagDrone One is an FGM only, whereas LEMI-026 is a complete instrument which may be used fully autonomously suspended to drone.

Table 1. Comparison of LEMI-026 and MagDrone One Main Technical Parameters**.**

Parameter	LEMI-026	MagDrone One
Measured range of the magnetic field	± 70000 nT	± 75000 nT
Frequency range	DC…100 Hz	No data
Sample rate	250 Hz	200 Hz
Noise level at 1 Hz	10 pT/√Hz	20 pT/√Hz
ADC (6 channels)	32 bits	24 bits
Tilt measurement range	±30°	No data
Tiltmeter resolution	0.01°	No data
Operating temperature range	-20… + 60 °C	-20 to +50 °C
Power supply voltage	5 ± 0.25 V	12 V
Maximal power consumption	< 1.2 W	6 W
Recording time with 1900 mAh internal battery	5 h	No data
GPS Receiver time stamps error maximal data rate	 <100 ns 10 Hz	No data
Digital interface	USB	Serial to USB
Volume of SD memory card	8 GB	No data
Internal memory	-	512 M
Weight	<1.25 kg	0.7 kg
Dimensions:	Electronic unit with sensor and battery Ø 96×270 mm	Electronic unit 205×105×45 mm Sensor Ø 35×365 mm

The external view of LEMI-026 FGM for drones use is given in Fig. 3 – both with weather-proof housing and without.

Fig. 3. External view of LEMI-026 magnetometer both with weather-proof housing (left) and without it (right).

4. Experimental Tests Results

The field tests were performed using two of the LEMI-026 magnetometers. The first problem which had to be investigated was magnetometer noise level (NL) in flight. The Fig. 4 shows that LEMI-026 magnetometer assembled with digital part has NL in stationary position below 30 picotesla, what is fairly good according to the modeling results (Figs. 1 - 2).

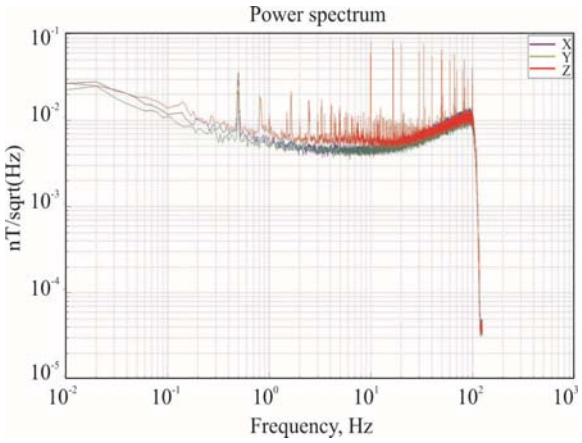

Fig. 4. Noise level of LEMI-026 magnetometer assembled with digital part in stationary position.

To estimate the FGM NL when mounted onboard the copter the data obtained at drone flight were submitted to spectral analysis (see Fig. 5). Here color plots are B_x, B_y, B_z components of the FGM and in black are given two components T_x, Ty of tiltmeter data. Necessary to mention that FGM spectra at Fig. 5 are not correct in the Earth frame system because axes azimuths are changing during the flight. More precisely, they have to be considered as FGM components in the frame system of the sensor. But we may accept them for further analysis because our goal here is to estimate what we may get from FGM on copter in movement.

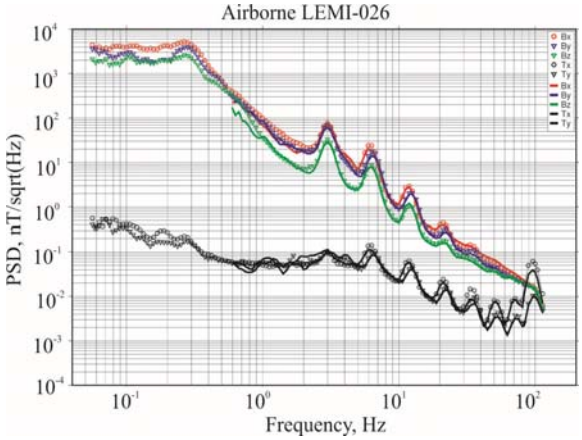

Fig. 5. Spectral analysis of LEMI-026 magnetometer noise level when mounted onboard drone at flight.

These data allow us to make following conclusions. First, strange set of oscillations with 3 Hz frequency and its harmonics are observed both in magnetometer and tiltmeter plots. We shall not comment them and only make an assumption that they are resulted by the mechanical oscillations of copter and FGM suspension system.

Next, the magnetic measurements in movement are used as it was mentioned above for aeromagnetic survey or buried objects detection. For the aeromagnetic survey variations in the period range more than 10 second are used. Analyzing data at the figure, we see that at the frequency 0.1 Hz signal fluctuations are around 2000 – 4000 nT, what is considerably more than any useful signal.

Nevertheless, let us try to analyze the obtained data in order to estimate whether it is possible to apply this method to aeromagnetic survey using the obtained during the flight data of components of vector of Earth's magnetic field and their spatial and temporal variations [25]. As it is seen from the Table 1, the sampling rate of FGM is 250 Hz, and GPS timing – 10 Hz. Because of this the first step was FGM data decimation to 10 Hz and then for every time moment the magnetic field module was calculated as:

$$F_f(t,x)\sqrt{B_x(t,x)^2 + B_y(t,x)^2 + \mathrm{B}_z(t,x)^2}, \quad (5)$$

where $F_f(t,x)$ is the vector of EMP induction for FGM in flight as function of time and space, $B_i(t,x)$ are the components of magnetic field induction vector.

For FGM in flight time and space variables are connected uniquely – to each moment of time responds its own position in space. At aeromagnetic survey, the spatial distribution of the EMP module under the studied area is searched; because of this the temporal variations have to be eliminated from the data. For this the data of a second – stationary FGM – were used, its decimation also was made and the file $F_b(t)$ was obtained. Then for every time moment the difference $F(x) = F_f(t,x) - F_b(t)$ was calculated as the data depending exclusively on spatial position of the flying FGM.

This value is plotted in Fig. 6 and corresponding area map with flight traces is given in Fig. 7.

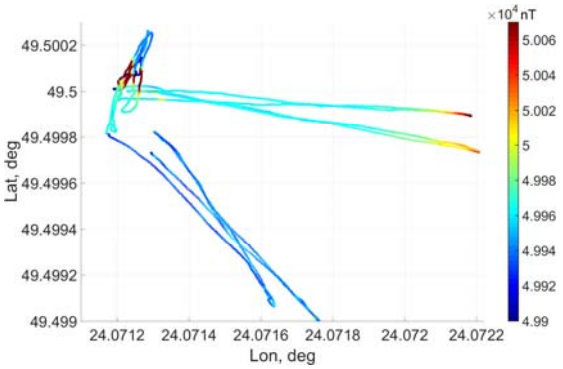

Fig. 6. Results of the magnetic field calculation as difference of the data of moving and stationary magnetometers.

Fig. 7. Test area map with flight traces corresponding to magnetic field data in Fig. 6.

From the comparison of both figures we may conclude that the tests were successful because namely at the places where enhanced intensity of the magnetic field was obtained the inspection revealed metalic bar (upper left part) and buried tube along the road (right part).

5. Conclusion

From the analysis above we may conclude that the parameters of the existing flux-gate magnetometers allow their using for magnetic survey with moving platforms. The electromagnetic interference from the drone motor and uncontrolled oscillations of drone and suspension are the main factors which limit the magnetometer sensitivity level. This problem can be solved by proper interference filtration and use of stabilized towed FGM construction. First results showed that FGM application for the search of metallic objects using scalar calculations seem to be satisfactory, but vector calculation results need further development. For this it is expected that matrix

method for FGM axes attitude reduction to geomagnetic frame can be successfully implemented for the electromagnetic sounding system, where the knowledge of sensor axes direction is important for data interpretation.

References

[1]. A. B. Broughton Edge, T. H. Laby, The Principles and Practice of Geophysical Prospecting, *Cambridge University Press*, 2012.

[2]. L. Dyson, C. Johnson, E. Heppell, M. Pieters, Archaeological evaluation of wetlands in the Planarch area of North West Europe, 2007. (http://agris.fao.org/agris-search/search.do?recordID=AV20120155498).

[3]. N. Linford, Archaeogeophysics: Applications and challenges for magnetic methods, in in *Proceedings of the Workshop on Soil Magnetism: Multidisciplinary Perspectives, Emerging Applications and New Frontiers: Report. ERDC Report,* 2009, pp. 35-36.

[4]. S. D. Stull, From west to east: current approaches to medieval archaeology, *Cambridge Scholars Publishing*, 2015.

[5]. Y. Das, Soil magnetism and landmine (metal) detectors, in in *Proceedings of the Workshop on Soil Magnetism: Multidisciplinary Perspectives, Emerging Applications and New Frontiers: Report. ERDC Report,* 2009, pp. 15-20.

[6]. L. R. Pasion, S. D. Billings, D. W. Oldenburg, Y. Li, N. Lhomme, Soil compensation techniques for the detection of buried metallic objects using electromagnetic sensors, in in *Proceedings of the Workshop on Soil Magnetism: Multidisciplinary Perspectives, Emerging Applications and New Frontiers: Report. ERDC Report,* 2009, p. 64.

[7]. E. Dobos, F. Carré, T. Hengl, H. I. Reuter, G. Tóth, Digital Soil Mapping as a support to production of functional maps, EUR 22123 EN, *Office for Official Publications of the European Communities*, Luxemburg, 2006.

[8]. T. Mayr, Digital Soil Mapping – spatial variability and prediction of soil properties, in in *Proceedings of the Workshop on Soil Magnetism: Multidisciplinary Perspectives, Emerging Applications and New Frontiers: Report. ERDC Report,* 2009, pp. 41-45.

[9]. L. D. McGinnis, M. D. Thompson, S. F. Miller, Environmental Geophysics: Buildings E5485, £5487, and E5489 Decommissioning - The 'Ghost Town' Complex, Aberdeen Proving Ground, Maryland, *Reclamation Engineering and Geosciences Section, Energy Systems Division, Argonne National Laboratory, Argonne,* The report, 1994.

[10]. J. W. E. Fassbinder, Geophysical Prospection: a Powerful Non-destructive Research Method for the Detection, Mapping and Preservation of Monuments and Sites, in *Proceedings of the 1st CEUR Workshop on The New Technologies for Aquileia*, Aquileia, Italy, May 2, 2011, pp. 1-9.

[11]. R. A. Viscarra Rossel, V. Adamchuk, Proximal soil sensing, in Precision Agriculture for Sustainability and Environmental Protection, M. Oliver, T. Bishop, B. Marchant (Eds.), *Routledge*, NY, 2013, pp. 15-28.

[12]. J. Hill, Civil engineering gives solar projects a firm foundation, *Solar Industry Magazine*, September 2015, pp. 1-11.

[13]. S. R. Evanko, D. A. Dzombak, Remediation of Metals-Contaminated Soils and Groundwater, Report TE-97-01, *Ground-Water Remediation Technologies Analysis Center*, *Carnegie Mellon University*, Pittsburgh, PA, 1997.

[14]. L. B. Ball, W. H. Kress, E. D. Anderson, A. P. Teeple, J. W. Ferguson, R. Charles, C. R. Colbert, Surface geophysical investigation of the areal and vertical extent of metallic waste at the former Tyson Valley Powder Farm near Eureka, *Scientific Investigations Report 2004–5208*, Missouri, Spring, 2004.

[15]. J. L. Gerberding, H. Frumkin, Ellenville scrap iron and metal, Public health assessment prepared, *Agency for Toxic Substances and Disease Registry,* Report, Ellenville, Ulster county, New York, EPA facility ID: NYSFN0204190, 2006.

[16]. K. F. Goddard, P. Wang, P. L. Lewin, S. G. Swingler, Detection and location of underground cables using magnetic field measurements, *Measurement Science and Technology*, Vol. 23, Issue 5, 2012.

[17]. X. Sun, Y. Hou, P. W. T. Pong, Underground Power Cable Detection and Inspection Technology Based on Magnetic Field Sensing at Ground Surface Level, *IEEE Transactions on Magnetics*, Vol. 50, Issue 7, July 2014.

[18]. Geotrace Pty Ltd (http://www.geotrace.com.au).

[19]. Geometrics, OYO Corporation (http://www.geometrics.com/geometrics-products/geometrics-magnetometers/).

[20]. SENSYS GmbH (http://www.sensysmagnetometer.com/en/magdrone-one.html).

[21]. V. Korepanov, Yu. Tsvetkov, Gradient magnetometer system for balloons, in *Proceedings of the 17th ESA Symposium on European Rocket and Balloon Programmes and Related Research*, Sandefjord, Norway, Vol. 590, 30 May – 2 June 2005, (ESA SP-590, August 2005), p. 443-450.

[22]. J. H. Scott, Electrical and magnetic properties of rock and soil, *Report 83-915,* Prepared in cooperation with the U.S. Air Force, 1983.

[23]. R. Fitzpatrick, Classical Electromagnetism, *Create Space Independent Publishing Platform*, 2016.

[24]. V. Korepanov, A. Marusenkov, Flux-Gate Magnetometers Design Peculiarities, *Surveys of Geophysics*, Vol. 33, Issue 5, 2012, pp. 1059–1079.

[25]. V. Korepanov, F. Dudkin, Magnetometer design for copters, in *Proceedings of the 2nd International Conference on Sensors Engineering and Electronics Instrumental Advances (SEIA' 2016),* 22-23 September 2016, Barcelona, Spain, pp. 138-139.
